HHS Public Access

Author manuscript

Sci Transl Med. Author manuscript; available in PMC 2017 August 23.

Published in final edited form as:

Sci Transl Med. 2017 June 14; 9(394): . doi:10.1126/scitranslmed.aal4508.

Donor pulmonary intravascular nonclassical monocytes recruit recipient neutrophils and mediate primary lung allograft dysfunction

Zhikun Zheng[1,*], **Stephen Chiu**[1,*], **Mahzad Akbarpour**[1], **Haiying Sun**[1], **Paul A. Reyfman**[2], **Kishore R. Anekalla**[2], **Hiam Abdala-Valencia**[2], **Daphne Edgren**[1], **Wenjun Li**[3], **Daniel Kreisel**[3], **Farida V. Korobova**[4], **Ramiro Fernandez**[1], **Alexandra McQuattie-Pimentel**[2], **Zheng J. Zhang**[1], **Harris Perlman**[2], **Alexander V. Misharin**[2], **GR Scott Budinger**[2], and **Ankit Bharat**[1,2,†]

[1]Department of Surgery, Northwestern University Feinberg School of Medicine, Chicago, IL 60611, USA

[2]Department of Medicine, Northwestern University Feinberg School of Medicine, Chicago, IL 60611, USA

[3]Department of Surgery, Washington University School of Medicine, Saint Louis, MO 63110, USA

[4]Department of Cell and Molecular Biology, Northwestern University Feinberg School of Medicine, Chicago, IL 60611, USA

Abstract

[†]Corresponding author. abharat@nm.org.
[*]These authors contributed equally to this work.

SUPPLEMENTARY MATERIALS

www.sciencetranslationalmedicine.org/cgi/content/full/9/394/eaal4508/DC1

Materials and Methods
Fig. S1. Cytokine analysis of the lung allograft.
Fig. S2. Representative gating strategy to evaluate the myeloid cell populations in the lungs.
Fig. S3. Perfusion of the heart-lung block.
Fig. S4. Effects of monocyte depletion strategies on the donor.
Fig. S5. Effects of donor clo-lip treatment on the 24-hour posttransplant allograft.
Fig. S6. Donor clo-lip treatment abrogates neutrophil influx after syngeneic lung transplant.
Fig. S7. Effects of CX3CR1 deletion on nonmonocyte cell populations in the lung and blood and on the posttransplant allograft.
Fig. S8. Effects of NR4A1 deletion on non-monocyte cell populations in the lung and blood and on the posttransplant allograft.
Fig. S9. All neutrophils were of recipient origin after 24 hours of reperfusion in the allograft.
Fig. S10. Representative gating strategy of GFP-expressing cells in the lungs of *Cx3cr1*$^{gfp/+}$ and *Cx3cr1*$^{gfp/gfp}$ mice.
Fig. S11. NCMs do not differentiate upon lipopolysaccharide challenge.
Fig. S12. Immunofluorescence microscopy of human lung biopsy from a patient experiencing PGD.
Fig. S13. Schematic to illustrate the role of pulmonary intravascular NCMs in mediating neutrophil infiltration and lung allograft injury.
Table S1. Primary data.
Movie S1. PBS-lip–treated control mice reveal profound neutrophil infiltration into the lung allograft after reperfusion.
Movie S2. Intravenous clo-lip treatment of the donors abrogates neutrophil infiltration into the allograft after reperfusion.
References (52–57)

Competing interests: The authors declare that they have no competing interests.

Author contributions: Z.Z., S.C., M.A., H.S., A.M.-P., R.F., P.A.R., K.R.A., H.A.-V., D.K., G.R.S.B., H.P., A.V.M., and A.B. contributed to study design, data collection and analysis, and manuscript writing. H.S., D.E., W.L., and A.B. contributed to data collection and analysis. F.V.K. performed electron microscopy and interpretation. Z.J.Z. provided support for microsurgeries.

Primary graft dysfunction is the predominant driver of mortality and graft loss after lung transplantation. Recruitment of neutrophils as a result of ischemia-reperfusion injury is thought to cause primary graft dysfunction; however, the mechanisms that regulate neutrophil influx into the injured lung are incompletely understood. We found that donor-derived intravascular nonclassical monocytes (NCMs) are retained in human and murine donor lungs used in transplantation and can be visualized at sites of endothelial injury after reperfusion. When NCMs in the donor lungs were depleted, either pharmacologically or genetically, neutrophil influx and lung graft injury were attenuated in both allogeneic and syngeneic models. Similar protection was observed when the patrolling function of donor NCMs was impaired by deletion of the fractalkine receptor CX3CR1. Unbiased transcriptomic profiling revealed up-regulation of MyD88 pathway genes and a key neutrophil chemoattractant, CXCL2, in donor-derived NCMs after reperfusion. Reconstitution of NCM-depleted donor lungs with wild-type but not MyD88-deficient NCMs rescued neutrophil migration. Donor NCMs, through MyD88 signaling, were responsible for CXCL2 production in the allograft and neutralization of CXCL2 attenuated neutrophil influx. These findings suggest that therapies to deplete or inhibit NCMs in donor lung might ameliorate primary graft dysfunction with minimal toxicity to the recipient.

INTRODUCTION

Primary graft dysfunction (PGD), which develops in more than 50% of lung allograft recipients, is the strongest risk factor for short-term mortality, early graft loss, and chronic rejection (1–4). Recipient neutrophils are the primary effector cells that are recruited to the allograft and lead to the development of PGD (5–11). After reperfusion, neutrophils are recruited from the circulation and extravasate into the alveolar space of the lung allograft where they undergo NETosis, resulting in tissue damage and further activating the inflammatory cascade (6, 12). Strategies to abrogate neutrophil influx and activation are expected to reduce PGD and improve short- and long-term outcomes in patients undergoing lung transplantation. This could be accomplished by systemic depletion of neutrophils before lung transplantation; however, this strategy is not clinically practical given the importance of neutrophils in host defense and pathogen clearance (7–11).

In both humans and mice, there are at least two distinct populations of peripheral blood monocytes, classical and nonclassical, which can be distinguished on the basis of their surface marker expression and behavior (13, 14). Classical monocytes (CMs) are known to leave the circulation in response to injury. Upon extravasation, CMs differentiate into inflammatory macrophages, playing important roles in the innate immune response to injury. Nonclassical monocytes (NCMs) adhere to the microvasculature, patrolling the endovascular space. NCMs have been shown to inhibit the metastatic spread of tumors and to promote the inflammatory response to viral infection, nephritis, and inflammatory arthritis via mechanisms that are incompletely understood (15–21). In previous studies of lung transplantation and ischemia-reperfusion, nonselective strategies to deplete monocytes reduced the severity of neutrophil egress into the lung (11). Because donor lungs are vigorously perfused to remove any intravascular cells before transplantation, these studies have focused on studying recipient-derived CMs and their role in the development of PGD (11). Although donor-derived lung-resident cells, such as alveolar macrophages, have also

been studied in the context of PGD, it was not until recently that our group and others reported the presence of donor-derived monocytes within lungs used in transplant (22, 23). As a result, detailed descriptions of these donor-derived monocytes and whether they play a role in the development of PGD have not yet been studied.

Here, we report that NCMs are present in murine donor lungs and are retained in the intravascular space despite vascular flushing. In murine models of syngeneic and clinically relevant allogeneic transplantation, pharmacologic or genetic depletion of NCMs in the donor lungs before transplantation markedly reduced the influx of neutrophils into the alveolar space and improved physiologic markers of lung allograft injury. Adoptive transfer of wild-type NCMs into mice deficient in NCMs restored neutrophil influx and lung injury after transplantation. Signaling through the adaptor protein MyD88 in NCMs was required to generate macrophage inflammatory protein-2 (CXCL2 or MIP-2), which was necessary for posttransplant neutrophil infiltration of the lung allograft. We confirmed that NCMs are retained in human donor lungs used in clinical transplantation and that the postperfusion allograft experiences a brisk neutrophil influx, similar to our murine model. These findings suggest that therapies that deplete or inhibit the function of NCMs might ameliorate PGD without impairing the host response to infection. Because these therapies can be selectively targeted to the donor lung, the toxicity to the recipient is predicted to be minimal.

RESULTS

Donor monocyte depletion confers protection against PGD after murine lung transplant

Given our previous unexpected finding of retained monocytes within the donor lung (22), we sought to test the hypothesis that depletion of donor-derived monocytes would ameliorate PGD using a reproducible and clinically relevant murine model of allogeneic lung transplantation. Because clodronate-loaded liposomes (clo-lip) efficiently deplete all monocyte subtypes in circulation (24, 25), we treated murine donors with clo-lip 24 hours before transplantation and measured the severity of PGD after transplantation (Fig. 1A). As shown in Fig. 1B, when donors were treated with clo-lip, gross and microscopic examination of the lung allograft showed no signs of lung injury and revealed preserved architecture without alveolar edema or hyaline membrane formation. In contrast, donors that received phosphate-buffered saline–loaded liposomes (PBS-lip) had signs of severe allograft injury and PGD development, including alveolar edema, capillaritis, and hyaline membrane development. Allografts from donors treated with clo-lip demonstrated normal oxygenation, whereas PBS-lip–treated mice had significantly impaired gas exchange (Fig. 1C). Native recipient lungs in both groups were preserved, and hearts revealed no damage. Donor clo-lip treatment protected against postreperfusion pulmonary edema, as indicated by multiple measures, including decreased wet-dry ratio (Fig. 1D), and capillary leak was determined using Evans blue dye extravasation (Fig. 1E). In addition, proinflammatory cytokines in bronchoalveolar lavage fluid were suppressed in clo-lip–treated donors compared to those treated with PBS-lip (fig. S1). Finally, to investigate whether clo-lip treatment had any detrimental long-term effects on the allograft function, we transplanted wild-type BALB/c lungs after clo-lip treatment of donors into wild-type C57BL/6 recipients and analyzed allograft function on day 30. To avoid allograft rejection resulting from de novo

alloimmunity, we administered costimulatory blockade using a combination of major histocompatibility complex (MHC)–related 1 and cytotoxic T lymphocyte–associated protein 4–immunoglobulin, as previously described (26–28). All lung allografts revealed a PaO_2 of >500 mmHg, indicative of normal function (mean, 543 ± 23). This demonstrated that donor monocyte depletion did not compromise long-term allograft function (Fig. 1C).

Intravenous clo-lip treatment selectively depletes pulmonary intravascular NCMs in donor lungs

Having observed the marked amelioration of PGD, we sought to determine the specific pulmonary myeloid cell populations affected by intravenous clo-lip treatment of the donors (Fig. 2A). Using a previously established protocol (22), we identified the myeloid populations in the perfused murine lungs (fig. S2). These murine lungs were perfused in a manner similar to that in human lung donors (see Materials and Methods for details). The perfusion of the lungs consistently eliminated circulating red blood cells (fig. S3). Donor lungs were found to have $CD45^+Ly6G^-NK1.1^-SiglecF^-CD64^-CD11b^+$ monocytes, in addition to other myeloid cell populations. Of these monocytes, both nonclassical $Ly6C^{low}$ $MHCII^-$ (3 to 5% of $CD45^+$) and classical $Ly6C^{high}$ $MHCII^{+/-}$(4 to 6% of $CD45^+$) were identified. NCMs comprised ~40 to 50% of total monocytes in flushed murine lungs. Intravenous injection of clo-lip completely depleted NCMs, but not CMs, in the donor lungs (Fig. 2, B and C). This was in contrast to blood and spleen where both subpopulations of monocytes were depleted (fig. S4A). Because liposomes administrated intravenously do not leave the intravascular compartment (17), intravenously administered clo-lip treatment only eliminates intravascular but not interstitial monocytes, indicating that NCMs and CMs are compartmentalized in the lung intravascular and interstitial spaces, respectively. In contrast, intravenous injection of anti-CCR2 antibodies led to depletion of only CMs, but not NCMs (Fig. 2, B and C), in the lungs. All other lung-resident myeloid cell populations were not affected by either clo-lip or anti-CCR2 treatment (fig. S4B). This indicated that the protection by donor clo-lip treatment against PGD after transplantation was due to selective depletion of pulmonary intravascular NCMs in the donor lungs.

Depletion of donor intravascular NCMs abrogates neutrophil influx after lung transplantation

Because PGD is mediated by neutrophils (29), we sought to determine whether depletion of donor pulmonary NCMs abrogated neutrophil influx after reperfusion of the allograft. We used LysM–GFP (green fluorescent protein) mice as recipients, which express GFP in neutrophils, allowing us to examine the dynamic influx of recipient neutrophils into the lungs and monitor in real time the rate of extravasation of recruited neutrophils after transplantation using intravital two-photon microscopy (Fig. 3A). Donors were treated intravaneously with clo-lip or PBS-lip as control 24 hours before transplantation. Two hours after reperfusion, lungs from PBS-lip–treated control donors demonstrated significant neutrophil extravasation (34.7 ± 4.94% of total neutrophils were extravascular). However, treatment of donors with clo-lip reduced neutrophil extravasation (9.43 ± 0.78% of total neutrophils; $P = 0.0072$) (Fig. 3, B to D, and movies S1 and S2). Thirty minutes later, the proportion of extravasated neutrophils in PBS-lip–treated control lung allografts continued to increase but much less so in clo-lip–treated donor lungs, which had proportionally fewer

extravasated neutrophils than control allografts (56.5 ± 4.17% versus 15.3 ± 0.64% of total neutrophils; $P = 0.0006$) (Fig. 3, E to G, and movies S1 and S2).

Because LysM-GFP mice can express GFP in other myeloid cells in addition to neutrophils, we used flow cytometry to confirm that pretreatment of donors before transplant with clo-lip leads to a significant suppression of neutrophil influx after allogeneic lung transplantation (Fig. 3H, group II). Although neutrophil influx was suppressed, we did not find any changes in the influx of other myeloid cells (fig. S5). At such early time points, it is generally accepted that there is no role for an alloimmune response in mediating neutrophil influx in naïve recipients (30). To confirm that alloimmunity did not play a role in neutrophil influx, we performed the same experiment using the syngeneic murine lung transplant model and found similar results (fig. S6). To eliminate the possibility that the neutrophil recruitment was mediated by donor CMs, we depleted them using anti-CCR2 antibodies before transplantation and found that neutrophil influx was unaltered in the absence of donor CMs (Fig. 3H, group III). Next, we eliminated the possibility of recipient-derived monocytes driving the neutrophil influx after lung allograft reperfusion by treating the recipients with clo-lip 48 hours before transplant, a procedure we have shown results in profound monocytopenia for 72 hours (17). Wild-type donor lungs transplanted into clo-lip–treated recipients were not protected from neutrophil infiltration after transplantation (Fig. 3H, group IV). Finally, we depleted donor CMs using anti-CCR2 antibodies and depleted all intravascular recipient monocytes with clo-lip 48 hours before transplantation. This treatment, which left only NCMs in the donor lungs, resulted in enhanced neutrophil infiltration after transplantation (Fig. 3H, group V).

Donor NCMs are necessary for neutrophil influx after reperfusion and development of PGD

We next confirmed the role of donor NCMs in neutrophil trafficking into the lungs after transplant with two independent genetic models (Fig. 4A). The fractalkine receptor CX3CR1 is not necessary for the formation of NCMs but is required for their patrolling function (19, 31). Consistently, we found that *Cx3cr1*$^{gfp/gfp}$ mice, which have a homozygous knock-in mutation of the fractalkine receptor, had preserved NCMs and other myeloid cells in the lungs under homeostasis (Fig. 4B and fig. S7). Heterozygous *Cx3cr1*$^{gfp/+}$ mice had levels of NCMs both in blood and in lung similar to wild-type mice (Fig. 4B and fig. S7B). When *Cx3cr1*$^{gfp/gfp}$ mice were used as lung donors, neutrophil influx was attenuated compared with *Cx3cr1*$^{gfp/+}$ donor lungs (Fig. 4B). *Cx3cr1*$^{gfp/gfp}$ donor lungs demonstrated preserved gas exchange and allograft architecture. In addition, the levels of proinflammatory cytokines were reduced in the bronchoalveolar lavage at 24 hours when *Cx3cr1*$^{gfp/gfp}$ donor lungs were used (fig. S7). We confirmed the role of CX3CR1 on donor NCMs by using neutralizing anti-CX3CR1 immunoglobulin G antibodies administered to the donor before the graft procurement and immediately after reperfusion. In contrast to isotype control antibodies, anti-CX3CR1 antibodies led to protection against neutrophil infiltration into the allograft similar to that observed in *Cx3cr1*$^{gfp/gfp}$ donor lungs (fig. S7).

The orphan nuclear receptor NR4A1 (also known as Nur77) is required for the differentiation of CMs into NCMs, and although these *Nr4a1*$^{-/-}$ mice develop normally, they lack NCMs (32). Consistent with these findings, we did not detect NCMs in perfused donor

lungs from *Nr4a1*$^{-/-}$ mice, but other myeloid cell populations were preserved (Fig. 4C&D and fig. S8A). Transplantation of *Nr4a1*$^{-/-}$ donor lungs into wild-type recipients was associated with reduced neutrophil recruitment and extravasation in the lung compared with allogeneic wild-type donors into wild-type recipients (Fig. 4D) and preserved allograft architecture (fig. S8).

Given these findings, we reasoned that reconstitution of *Nr4a1*$^{-/-}$ mice (B6 background) with isogenic *Cx3cr1*$^{gfp/+}$ NCMs (B6 background) should allow us to reverse the protection conferred by the loss of NR4A1. Use of functional *Cx3cr1*$^{gfp/+}$cells, which have the GFP on NCMs, allowed us to confirm successful engraftment into the NR4A1 mice and track them after transplantation. Adoptive transfer of NCMs restored the number of these cells in the NR4A1 murine lungs in the same spatial distribution (Fig. 4D). There was no difference in the other myeloid cell population in the reconstituted NR4A1 donor lungs (fig. S8D). When these NR4A1-deficient lungs were reconstituted with *Cx3cr1*$^{gfp/+}$ NCMs and then used as donors, neutrophil influx after transplantation was restored (Fig. 4D). All neutrophils at 24 hours were of recipient origin (fig. S9), consistent with the rapid recipient-derived neutrophil influx observed during two-photon imaging of LysM-GFP recipients.

Pulmonary NCMs reside in the intravascular space

The selective and complete depletion of murine pulmonary NCMs with clo-lip suggested that they are present only in the intravascular space under homeostasis. To confirm the anatomical localization of NCMs in the lung tissue, we further studied the *Cx3cr1*$^{gfp/+}$ reporter mouse. Two-photon imaging of murine Cx3cr1$^{gfp/+}$ lungs revealed intravascular cells with green fluorescence (Fig. 5A). In addition, there were interstitial GFP^{+} cells that resembled dendritic cells and macrophages. Flow cytometry revealed that GFP^{+} cells were predominantly composed of NCMs and CMs along with a small fraction of dendritic cells, macrophages, and natural killer (NK) cells (fig. S10). To further characterize the morphology of these cells, we evaluated the intravascular GFP^{+} cells in the lungs using electron microscopy with immunolabeling. Lungs were flushed to eliminate unbound intravascular cells from *Cx3cr1*$^{gfp/+}$ mice and then labeled using gold nanoparticles conjugated to anti-GFP antibodies. Intravascular cells attached to the endothelium were found to have gold deposition and the morphology of mononuclear phagocytes, consistent with intravascular monocytes (Fig. 5B). Myeloid populations from flushed lungs were then sorted using flow cytometry and imaged. The in situ NCMs resembled flow-sorted NCMs but not alveolar macrophages, CMs, or NK cells (Fig. 5B). Specifically, pulmonary NCMs were smaller than CMs and larger than NK cells and had a nucleus-to-cytoplasm ratio higher than CMs but lower than NK cells. Both CMs and NCMs were rich in mitochondria, vacuoles, and endoplasmic reticulum, consistent with the known properties of monocytes as phagocytes and drivers of inflammatory responses, as previously described (18). We further imaged the *Cx3cr1*$^{gfp/+}$ lung allografts using electron microscopy at 4 hours after reperfusion to confirm the persistence of donor-derived NCMs after ischemia-reperfusion. As shown in Fig. 5C, we found that gold-labeled NCMs were bound to the endothelium, near areas of exposed, thickened basement membrane and endothelial cell blebbing.

We then used intravenous and intratracheal compartmental staining (33, 34) to confirm that NCMs in homeostatic lungs are in the intravascular space and to characterize their response to intratracheal lipopolysaccharide, a bacterial cell wall motif. All NCMs were stained with intravenously injected anti-CD45 antibodies but not with antibodies injected into the trachea (Fig. 5D). The intratracheal staining was effective because all alveolar macrophages were stained for tracheally administered anti-CD45 (Fig. 5D). Intratracheal lipopolysaccharide led to migration of CMs, but not NCMs, into the alveolar space (Fig. 5E). We then precluded the possibility of NCMs differentiating into interstitial CMs or alveolar macrophages after intratracheal lipopolysaccharide administration. Toward this, we adoptively transferred NCMs isolated from wild-type B6-CD45.1 hosts into *Nr4a1*$^{-/-}$ hosts (B6-CD45.2 background), and after engraftment of the NCMs into the lungs, we challenged the reconstituted *Nr4a1*$^{-/-}$ hosts with intratracheal lipopolysaccharide. None of the CMs or alveolar macrophages were found to be CD45.1-positive, confirming that NCMs do not extravasate in response to intratracheal lipopolysaccharide (fig. S11). Furthermore, treatment of wild-type hosts with intravenous clo-lip did not affect neutrophil influx into the lungs after intratracheal administration of lipopolysaccharide (Fig. 5E), suggesting that depletion of NCMs in the donor lungs might not affect recipient's defense against respiratory pathogens. Together, these findings indicate that NCMs in native lungs exist in the intravascular space, and although CMs can move into the alveoli in response to intratracheal pathogen stimuli, NCMs remain intravascular.

Transcriptomic profiling reveals up-regulation of MyD88 pathway genes and neutrophil chemoattractants in donor NCMs after reperfusion

Having confirmed that donor NCMs were necessary and sufficient for recruiting neutrophils into the allograft, which leads to PGD, we then sought to investigate the mechanisms by which they recruited neutrophils. To do so, we used the *Cx3cr1*$^{gfp/+}$ reporter mouse, which allowed for flow sorting of donor-origin NCMs before and after allogeneic transplantation (Fig. 6, A and B). Donor-origin NCMs isolated during the resting state of the donor and at different time points after transplantation underwent unbiased whole-transcriptome analysis by RNA sequencing (Fig. 6, C and D). Given one previous report of NCMs up-regulating Toll-like receptor 7 (TLR7) transcripts and initiating neutrophil recruitment in a model of nephritis (18), we queried TLR pathways using KEGG PATHWAY mapping (www.kegg.jp/kegg/pathway.html). We found that genes from the TLR2/CD14 and MYD88 pathways were up-regulated along with transcripts for MIP-2 (or CXCL2), a potent neutrophil chemoattractant (Fig. 6E). Together, this suggested that TLR signaling and production of neutrophil chemoattractants, such as CXCL2, by donor NCMs might be responsible for neutrophil recruitment after lung transplantation.

Donor NCMs produce CXCL2 in a TLR-dependent manner to recruit recipient neutrophils

All TLRs initiate their signaling cascade via their adaptor proteins, MyD88 and/or TRIF (Toll/interleukin-1 receptor domain–containing adapter-inducing interferon-β). Supported by the data from our unbiased transcriptome analysis, we used the dual-knockout *Myd88*$^{-/-}$/*Trif*$^{-/-}$ mouse in a series of adoptive transfer experiments (Fig. 7A). When *Myd88*$^{-/-}$/*Trif*$^{-/-}$ mice were used as donors, there was reduced neutrophil infiltration in the allograft compared with wild-type donor lungs (Fig. 7B). These findings suggested that TLR signaling in the

donor allograft, either in the stroma or in the myeloid cells, was important for initiation of neutrophil recruitment. Previous studies have shown that TLR-dependent activation of stroma and endothelium can recruit monocytes and promote inflammation (18). However, the precise cell types and underlying mechanisms are unknown. To specifically investigate the role of TLR signaling in NCMs, we reconstituted clo-lip–treated donor lungs with NCMs from either wild-type or *Myd88*/*Trif*$^{-/-}$ mice ex vivo after harvest and then used these reconstituted grafts in transplant (Fig. 7A). As shown in Fig. 7B, reconstitution with wild-type NCMs, but not TLR-deficient NCMs, restored neutrophil influx into the transplanted lungs, indicating that TLR signaling in NCMs is necessary for neutrophil recruitment.

CXCL2 has been shown to play an important role in neutrophil chemotaxis and extravasation in many tissues (35, 36) and has also emerged as a crucial chemokine in the recruitment of neutrophils to the lungs (9, 37–40). Given that *Cxcl2* transcripts were up-regulated in donor-derived NCMs after transplant (Fig. 6E), we tested whether MyD88/TRIF signaling was necessary for the production of CXCL2. We first transplanted either wild-type or *Myd88*/*Trif*$^{-/-}$ donor lungs into wild-type allogeneic recipients. Two hours after reperfusion, donor-derived NCMs were isolated from the allograft, and *Cxcl2* mRNA transcript abundance was analyzed. We found that NCMs from wild-type donors up-regulated *Cxcl2*, but NCMs from *Myd88*/*Trif*$^{-/-}$ donors did not (Fig. 7C). At the same time, analysis of allograft pulmonary vein blood showed increased CXCL2 levels after transplant of wild-type donor lungs. However, CXCL2 levels were suppressed if NCMs were depleted in donor lungs with clo-lip or if *Nr4a1*$^{-/-}$ and *Myd88*/*Trif*$^{-/-}$ donor lungs were used (Fig. 7D). Neutralizing CXCL2 using anti-CXCL2 antibodies at the time of transplantation, but not isotype control, attenuated neutrophil influx in NCM-sufficient donors (Fig. 7E). Furthermore, the allograft function was significantly improved in mice receiving anti-CXCL2 antibodies compared to isotype control (PaO_2, 469.7 ± 27.3 mmHg versus 200.7 ± 6.2 mmHg; $P = 0.0007$). Collectively, these data indicate that NCMs induce the recruitment of neutrophils by producing CXCL2 in a MyD88/TRIF-dependent fashion.

NCMs persist in the vasculature of human donor lungs procured for transplantation

Ly6C^{low}CX3CR1^{hi}CCR2^{-} murine NCMs are analogous to human CD14^{dim}CD16^{++} monocytes (41). To determine whether our findings could apply to human lung transplantation, we evaluated the presence of NCMs in human donor lungs procured for lung transplantation using established protocols (22). These lungs were flushed using both antegrade and retrograde flush as is common in clinical practice (see Materials and Methods for details). CD45^{+}CD15^{-}HLADR^{+}CD11b^{+}CD169^{-}CD206^{-} monocytes comprised 4 to 8% of resident lung myeloid cells. Of these, NCMs (CD14^{dim}CD16^{++}) comprised 3 to 14%, CMs (CD14^{+}CD16^{-}) comprised 62 to 83%, and intermediate monocytes (CD14^{+}CD16^{+}) comprised 12 to 19% (Fig. 8A). The population of NCMs detected before reperfusion was stable at 90 min after reperfusion (Fig. 8B). There was a rapid increase in the number of neutrophils (Fig. 8B), similar to the murine allografts (Fig. 3). We used immunofluorescence of perfused human donor lungs and detected intravascular NCMs (Fig. 8C). These cells persisted immediately after reperfusion (Fig. 8D) and were observed in the regions of neutrophil aggregation (fig. S12). Together, these studies confirmed the presence of NCMs

in human donor lungs used in clinical transplant and verified the clinical relevance of our murine model.

DISCUSSION

Here, we show that donor-derived intravascular pulmonary NCMs are the primary drivers of neutrophil recruitment into the lung during ischemia-reperfusion injury and cause PGD after lung transplant. These findings fundamentally change our understanding of the role of monocytes in the development of early ischemia-reperfusion injury and conclusively identify donor-derived NCMs as the culprit myeloid cell. Genetic loss of TLR signaling in NCMs through simultaneous deletion of MyD88 and TRIF prevented NCM-mediated neutrophil influx into the lung after transplantation, in part, by preventing the release of the neutrophil chemokine CXCL2. Our studies of human lungs used in clinical transplantation confirmed that NCMs persist in donor lungs and that there is a brisk neutrophil influx into the allograft, parallel to our murine model. Together, our data suggest that targeting NCMs in the donor lung before transplantation might reduce the severity of PGD, the principal predictor of poor outcomes immediately after lung transplantation and the strongest risk factor for chronic allograft rejection (3, 4). Because these therapies could be applied to the donor lung before transplantation, it is unlikely that they will be toxic to the recipient.

Distinct populations of circulating monocytes have been recently identified on the basis of surface marker expression and morphology: classical and nonclassical (13, 14, 42). CMs are a well-studied population of circulating bone marrow–derived cells that migrate into tissues in response to injury. In mice, these cells are identified by their high-level expression of Ly6C, CD62L, and CCR2, which are all involved in homing to sites of injury, and intermediate expression of CX3CR1 (42). At a steady state, CMs differentiate into NCMs, losing expression of Ly6C and CD62L while up-regulating the expression of the fractalkine receptor CX3CR1 and of CD43, a sialomucin involved in leukocyte adhesion (43). NCMs adhere to the vascular wall where they “patrol” the vascular space, sometimes crawling against the flow of blood. The function of NCMs in homeostasis and pathophysiology has been a recent topic of intense study, and in the context of inflammation, NCMs have been shown to remove apoptotic endothelial cells and other vascular debris (42). Analogous populations of CMs and NCMs have been observed in humans distinguished by high and low expression of CD14, respectively (13, 14, 42).

In the context of lung transplantation, circulating CMs in the recipient have been previously implicated in the development of PGD and models of ischemia-reperfusion injury, such as hilar clamping (11). We believe that interpretations from these studies might have been confounded by the lack of sufficient phenotypic markers to distinguish CMs and NCMs and the inability to distinguish between vascular-adherent and circulating cells. In addition, it has been assumed that circulating monocytes are depleted from the donor lung through vigorous perfusion before transplant. Therefore, we were surprised to find NCMs in biopsies from human lung allografts obtained immediately before transplant, a finding that was subsequently confirmed by other groups (22, 23). Using murine models, including the *Cx3cr1*$^{gfp/+}$ reporter, which allows for the tracking of functional monocytes (44), we were able to show that the population of intravascular monocytes retained in the lung after

perfusion was exclusively composed of NCMs and was completely depleted after the administration of clo-lip. Electron micrographs of the postreperfusion lung showed that donor NCMs were scattered throughout the vasculature and in areas of exposed basement membrane, suggesting that they mediated their effects either through a direct binding interaction with the vasculature or through its underlying basement membrane, or perhaps through a paracrine release of chemokines or cytokines.

To determine whether NCMs in the donor lung play a causal role in PGD, we depleted the NCMs before transplantation in our murine model. This resulted in a marked reduction in neutrophil egress into the alveolar space and a marked improvement in all of the physiologic markers of PGD. Although we observed neutrophil egress into the alveolus in regions of the lung immediately adjacent to NCMs during intravital imaging, we also noted neutrophil egress in regions where NCMs were not present. This might result from limitations of currently available imaging techniques or suggest a mechanism in which signaling in the NCMs triggers the release of soluble chemokines or cytokines to affect generalized neutrophil egress. The latter hypothesis is consistent with our finding that NCMs increased the transcription of *Cxcl2* after transplantation and that the administration of neutralizing anti-CXCL2 markedly attenuated neutrophil influx after transplantation. This mechanism may also explain the marked change in phenotype we observed after depletion of the relatively rare population of NCMs.

Previously, investigators attributed the reductions in neutrophil influx they observed in recipient mice treated with intravenous clo-lip immediately before transplantation to the depletion of CMs in the recipient (11). However, we found that this strategy also depletes donor-derived NCMs in the allograft. By differentially administering cytotoxic antibodies directed against CCR2 (to selectively target pulmonary CMs) and clo-lip (to target pulmonary NCMs), we were able to show that the protection conferred by the administration of clo-lip to the recipient was attributable to the depletion of NCMs in the donor. Depleting monocytes in the recipient without depleting NCMs in the donor led to an unexpected increase in neutrophil recruitment into the lung. Ischemia-reperfusion injury causes PGD in more than 50% of patients after human lung transplantation (1–4), but not all recipients experience PGD. We postulate that some of the heterogeneity in the development of PGD after human lung transplant could be explained by the number or viability of NCMs in the donor lung at the time of transplantation and perhaps the number and function of CMs in the recipient. Using fate-mapping techniques, previous studies have indicated that the life span of NCMs is about 2 days (45). However, if CMs are depleted, NCMs survive for up to 5 days (45). Hence, variability in the number of NCMs and their ability to survive and perpetuate injury within donor lungs might affect development of human PGD.

The orphan nuclear receptor NR4A1 has been shown to be required for the differentiation of CMs into NCMs (32). NR4A1-deficient mice lack NCMs in the circulation and tissues and therefore provide a genetic approach to determine the importance of donor-derived NCMs in the development of PGD. We found that neutrophil influx into the engrafted lung after transplant and the severity of the resulting PGD were markedly reduced when lungs from *Nr4a1*$^{-/-}$ donors were transplanted into wild-type mice. This protection is not attributable to a function of NR4A1 independent of its inhibition of NCM differentiation, because the

adoptive transfer of functional NCMs into *Nr4a1*$^{-/-}$ mice before transplant restored neutrophil influx into the allograft. Further genetic evidence supporting the importance of NCMs in neutrophil influx comes from mice lacking the fractalkine receptor CX3CR1. In some models, CX3CR1 has been suggested to be required for the patrolling behavior of NCMs along the vascular endothelium, whereas in a kidney injury model, CX3CR1 was shown to be required for neutrophil influx independent of any effect on their patrolling behavior (20, 46, 47). Similar to NR4A1 deletion, we found that donor lungs from mice deficient in CX3CR1 showed marked attenuation of neutrophil influx after transplantation. Our findings did not suggest a role for CX3CR1 in the adherence of NCMs to the pulmonary vasculature because the number of NCMs in donor lungs from *Cx3cr1*$^{gfp/gfp}$ mice was similar to controls. Although it could be argued in our pharmacologic depletion studies that donor lungs retained clo-lip and depleted recipient blood monocytes upon reperfusion, liposomes do not cross capillary barriers and are not known to adhere to pulmonary vasculature (48), making this an unlikely scenario. In addition, we found that genetic deletion of either CX3CR1 or NR4A1 in the donor lung prevented neutrophil influx into the lung after transplantation, and reconstitution of either clodronate-depleted or *Nr4a1*$^{-/-}$ donor lungs with flow-sorted NCMs from wild-type mice restored neutrophil influx. These data demonstrate that donor-derived pulmonary NCMs are necessary and sufficient for initiating neutrophil influx after lung transplantation independent of potential off-target effects of clo-lip depletion.

Our group and others have previously shown that neutrophil recruitment, in certain models of inflammation, including the serum-induced model of rheumatoid arthritis and a model of autoimmune kidney injury, is dependent on NCMs, which may be activated through TLR7 ligation (18, 49). Guided by these previous reports, we examined the role of TLR signaling in NCMs in mediating the egress of neutrophils during ischemia-reperfusion injury. We found that transcripts for genes involved in TLR signaling through its downstream adaptors were up-regulated but found that in this model, TLR2 and its co-receptor CD14 were up-regulated, whereas TLR7 was not. In confirmatory studies, we used mice doubly deficient in MyD88 and TRIF. One or both of these proteins are required for signaling through all of the described TLRs (50). We found that transplantation of lungs from these mice into wild-type recipients reduced neutrophil egress into the lung after transplantation to a level similar to that observed in allografts depleted of NCMs. Furthermore, reconstitution of wild-type clo-lip–treated donor lungs with flow-sorted NCMs from *MyD88/Trif*$^{-/-}$ mice failed to restore neutrophil recruitment into the lung, whereas reconstitution using NCMs from wild-type mice did. However, NCMs did not mediate neutrophil influx in response to lipopolysaccharide, suggesting that they are not activated through TLR4 pathway but through a damage-associated molecular pattern-sensing pathway. Notably, our studies of NCM depletion using pretreatment with clo-lip before lipopolysaccharide challenge differ from previous studies that used clo-lip to induce depletion of circulating monocytes after lipopolysaccharide administration (48). Hence, pulmonary intravascular NCMs may play a broader role in mediating sterile, but not pathogen-induced, lung inflammation, and their transient depletion may not compromise host pathogen defense.

Our studies identify NCMs as the causal cell type responsible for ischemia-reperfusion injury through the production of neutrophil chemoattractants. One of these, CXCL2, has

been shown to play an important role in neutrophil recruitment (37–40). Unbiased whole transcriptome analysis and confirmatory quantitative polymerase chain reaction showed that *Cxcl2* transcripts were up-regulated nearly 10-fold after graft reperfusion. Accordingly, we examined the expression of *Cxcl2* in flow-sorted NCMs from wild-type and *MyD88/Trif*$^{-/-}$ donor mice after transplantation and found that *Cxcl2* mRNA was markedly elevated after transplant in the wild-type, but not *Myd88*$^{-/-}$/*Trif*$^{-/-}$, donor NCMs. This could represent a scenario in which stored CXCL2 is immediately released upon activation, and the observed transcription is occurring in response to replenish stores and continually produce the chemokine because of ongoing TLR signaling. Consistent with this hypothesis, parallel differences were observed in the levels of CXCL2 in the pulmonary veins from the donor lungs after transplant.

We show that the strategies currently used to perfuse lung allografts leave a population of NCMs in the vasculature of the human lung. In mice, this retained population is sufficient to mediate neutrophil egress into the lung after transplantation. These findings have important potential clinical applications. Bisophosphonates, such as clodronate, have a long history of safety in humans (51), and pharmacologic procedures to encapsulate drugs into liposomes that facilitate uptake by macrophages can be made readily available. Although the effects of these medications may preclude their administration to the recipient in the perioperative period after transplant, administration of an NCM-depleting agent to the donor lung at the time of procurement or ex vivo, prior to implantation, is predicted to be safe and feasible. Safety might be further improved through strategies that detach NCMs from the vasculature without killing them, allowing them to be efficiently flushed from the pulmonary vasculature, and may transiently prevent the recruitment of recipient-derived NCMs after implantation. Alternatively, the activation of NCMs in the donor lung might be inhibited through the use of TLR antagonists. Finally, chemokines or cytokines released from NCMs after transplantation might be targeted in the recipient, which could dampen neutrophil recruitment by recipient-derived NCMs recruited to the allograft after transplantation (fig. S13), but would have to be modulated closely to prevent adverse effects of such a strategy.

Together, these findings represent a significant advance in our understanding of the role of monocytes during inflammation and a fundamental change in our comprehension of the pathophysiology of ischemia-reperfusion injury and PGD with important clinical implications. Our findings in a murine lung transplant model suggest that targeting these NCMs in the donor lung before transplantation will likely reduce the disease burden of PGD after lung transplantation.

MATERIALS AND METHODS

Study design

The objective of this study was to determine the role of donor-derived NCMs in the pathogenesis of primary lung allograft dysfunction. Flow cytometry and immunofluorescence microscopy were used to identify NCMs in donor human lungs before and after reperfusion. Murine single-lung transplant was used as a model of human transplantation and to test the effects of donor and recipient treatments, genetic deletion, and cell adoptive transfer. Intravital two-photon microscopy and flow cytometry were used to

measure the influx of inflammatory cell populations into the lung. Compartmental staining for flow cytometry, immunofluorescence two-photon microscopy, and immunoelectron microscopy were used to anatomically localize NCMs in the intravascular space. To identify activation pathways and proinflammatory chemokines released by NCMs, RNA sequencing was performed on FACS (fluorescence-activated cell sorter)–sorted donor-derived NCMs in the allograft early after transplant. Genetic deletion of MYD88 and TRIF and measurement of CXCL2 in the posttransplant allograft were performed on the basis of their identification as candidate activation pathways and as an identified neutrophil chemokine during analysis of whole transcriptome data. In an independent set of experiments, to examine the effects of NCMs on the host's ability to respond to pathogen, mice depleted of NCMs were treated with intratracheal instillation of lipopolysaccharide to model lung injury induced by a Gram-negative organism. In vivo experiments represent pooled results of at least two repeated experiments, unless otherwise indicated. Details of all protocols and primary data for experiments where $n < 20$ (table S1) are provided in the Supplementary Materials.

Statistical analysis

All data are means ± SEM. Comparison between two groups was performed by unpaired t tests with Holm-Šidák correction for multiple comparisons, unless otherwise noted in the figure legends.

Supplementary Material

Refer to Web version on PubMed Central for supplementary material.

Acknowledgments

We thank S. Swaminathan for assistance with multicolor flow cytometry, C. Arvanitis for technical assistance with multiphoton imaging, and E. Susan for administrative assistance and for formatting the manuscript.

Funding: This study was supported by NIH T32 DK077662 and American Society for Transplant Surgery (to S.C.); NIH P01 AG049665, NIH P01 HL071643, and Department of Defense PR141319 (to G.R.S.B., H.P., and A.V.M.); and NIH HL125940, Thoracic Surgery Foundation, American Lung Association, and Society of University Surgeons (to A.B.). The Northwestern University Flow Cytometry Core Facility is supported by National Cancer Institute (NCI) Cancer Center Support Grant (CCSG) (NCI CA060553). Flow cytometry cell sorting was performed on a BD FACSAria SORP system, purchased through the support of NIH 1S10OD011996-01. Imaging work performed at the Northwestern University Center for Advanced Microscopy was generously supported by NCI CCSG P30 CA060553 awarded to the Robert H. Lurie Comprehensive Cancer Center. Multiphoton microscopy was performed on a Nikon A1R multiphoton microscope, acquired through the support of NIH 1S10OD010398-01.

REFERENCES AND NOTES

1. Porteous MK, Diamond JM, Christie JD. Primary graft dysfunction: Lessons learned about the first 72 h after lung transplantation. Curr Opin Organ Transplant. 2015; 20:506–514. [PubMed: 26262465]
2. Christie JD, Carby M, Bag R, Corris P, Hertz M, Weill D. ISHLT Working Group on Primary Lung Graft Dysfunction. Report of the ISHLT Working Group on Primary Lung Graft Dysfunction part II: Definition. A consensus statement of the International Society for Heart and Lung Transplantation. J Heart Lung Transpl. 2005; 24:1454–1459.
3. Bharat A, Kuo E, Steward N, Aloush A, Hachem R, Trulock EP, Patterson GA, Meyers BF, Mohanakumar T. Immunological link between primary graft dysfunction and chronic lung allograft rejection. Ann Thorac Surg. 2008; 86:189–195. [PubMed: 18573422]

4. Daud SA, Yusen RD, Meyers BF, Chakinala MM, Walter MJ, Aloush AA, Patterson GA, Trulock EP, Hachem RR. Impact of immediate primary lung allograft dysfunction on bronchiolitis obliterans syndrome. Am J Respir Crit Care Med. 2007; 175:507–513. [PubMed: 17158279]
5. Belperio JA, Keane MP, Burdick MD, Londhe V, Xue YY, Li K, Phillips RJ, Strieter RM. Critical role for CXCR2 and CXCR2 ligands during the pathogenesis of ventilator-induced lung injury. J Clin Invest. 2002; 110:1703–1716. [PubMed: 12464676]
6. Ley K, Laudanna C, Cybulsky MI, Nourshargh S. Getting to the site of inflammation: The leukocyte adhesion cascade updated. Nat Rev Immunol. 2007; 7:678–689. [PubMed: 17717539]
7. Tsai KS, Grayson MH. Pulmonary defense mechanisms against pneumonia and sepsis. Curr Opin Pulm Med. 2008; 14:260–265. [PubMed: 18427251]
8. Tate MD, Deng Y-M, Jones JE, Anderson GP, Brooks AG, Reading PC. Neutrophils ameliorate lung injury and the development of severe disease during influenza infection. J Immunol. 2009; 183:7441–7450. [PubMed: 19917678]
9. Belperio JA, Keane MP, Burdick MD, Gomperts BN, Xue YY, Hong K, Mestas J, Zisman D, Ardehali A, Saggar R, Lynch JP III, Ross DJ, Strieter RM. CXCR2/CXCR2 ligand biology during lung transplant ischemia-reperfusion injury. J Immunol. 2005; 175:6931–6939. [PubMed: 16272353]
10. Zarbock A, Allegretti M, Ley K. Therapeutic inhibition of CXCR2 by Reparixin attenuates acute lung injury in mice. Br J Pharmacol. 2008; 155:357–364. [PubMed: 18587419]
11. Kreisel D, Nava RG, Li W, Zinselmeyer BH, Wang B, Lai J, Pless R, Gelman AE, Krupnick AS, Miller MJ. In vivo two-photon imaging reveals monocyte-dependent neutrophil extravasation during pulmonary inflammation. Proc Natl Acad Sci USA. 2010; 107:18073–18078. [PubMed: 20923880]
12. Sørensen OE, Borregaard N. Neutrophil extracellular traps—The dark side of neutrophils. J Clin Invest. 2016; 126:1612–1620. [PubMed: 27135878]
13. Ziegler-Heitbrock L, Ancuta P, Crowe S, Dalod M, Grau V, Hart DN, Leenen PJ, Liu Y-J, MacPherson G, Randolph GJ, Scherberich J, Schmitz J, Shortman K, Sozzani S, Strobl H, Zembala M, Austyn JM, Lutz MB. Nomenclature of monocytes and dendritic cells in blood. Blood. 2010; 116:e74–e80. [PubMed: 20628149]
14. Chiu S, Bharat A. Role of monocytes and macrophages in regulating immune response following lung transplantation. Curr Opin Organ Transplant. 2016; 21:239–245. [PubMed: 26977996]
15. Hanna RN, Cekic C, Sag D, Tacke R, Thomas GD, Nowyhed H, Herrley E, Rasquinha N, McArdle S, Wu R, Peluso E, Metzger D, Ichinose H, Shaked I, Chodaczek G, Biswas SK, Hedrick CC. Patrolling monocytes control tumor metastasis to the lung. Science. 2015; 350:985–990. [PubMed: 26494174]
16. Cros J, Cagnard N, Woollard K, Patey N, Zhang S-Y, Senechal B, Puel A, Biswas SK, Moshous D, Picard C, Jais J-P, D'Cruz D, Casanova J-L, Trouillet C, Geissmann F. Human $CD14^{dim}$ monocytes patrol and sense nucleic acids and viruses via TLR7 and TLR8 receptors. Immunity. 2010; 33:375–386. [PubMed: 20832340]
17. Misharin AV, Cuda CM, Saber R, Turner JD, Gierut AK, Haines GK III, Berdnikovs S, Filer A, Clark AR, Buckley CD, Mutlu GM, Budinger GR, Perlman H. Nonclassical $Ly6C^{-}$ monocytes drive the development of inflammatory arthritis in mice. Cell Rep. 2014; 9:591–604. [PubMed: 25373902]
18. Carlin LM, Stamatiades EG, Auffray C, Hanna RN, Glover L, Vizcay-Barrena G, Hedrick CC, Cook HT, Diebold S, Geissmann F. *Nr4a1*-dependent $Ly6C^{low}$ monocytes monitor endothelial cells and orchestrate their disposal. Cell. 2013; 153:362–375. [PubMed: 23582326]
19. Collison JL, Carlin LM, Eichmann M, Geissmann F, Peakman M. Heterogeneity in the locomotory behavior of human monocyte subsets over human vascular endothelium in vitro. J Immunol. 2015; 195:1162–1170. [PubMed: 26085686]
20. Auffray C, Fogg D, Garfa M, Elain G, Join-Lambert O, Kayal S, Sarnacki S, Cumano A, Lauvau G, Geissmann F. Monitoring of blood vessels and tissues by a population of monocytes with patrolling behavior. Science. 2007; 317:666–670. [PubMed: 17673663]
21. Nahrendorf M, Swirski FK, Aikawa E, Stangenberg L, Wurdinger T, Figueiredo J-L, Libby P, Weissleder R, Pittet MJ. The healing myocardium sequentially mobilizes two monocyte subsets

with divergent and complementary functions. J Exp Med. 2007; 204:3037–3047. [PubMed: 18025128]

22. Bharat A, Bhorade SM, Morales-Nebreda L, McQuattie-Pimentel AC, Soberanes S, Ridge K, DeCamp MM, Mestan KK, Perlman H, Budinger GR, Misharin AV. Flow cytometry reveals similarities between lung macrophages in humans and mice. Am J Respir Cell Mol Biol. 2016; 54:147–149. [PubMed: 26274047]
23. Desch AN, Gibbings SL, Goyal R, Kolde R, Bednarek J, Bruno T, Slansky JE, Jacobelli J, Mason R, Ito Y, Messier E, Randolph GJ, Prabagar M, Atif SM, Segura E, Xavier RJ, Bratton DL, Janssen WJ, Henson PM, Jakubzick CV. Flow cytometric analysis of mononuclear phagocytes in nondiseased human lung and lung-draining lymph nodes. Am J Respir Crit Care Med. 2016; 193:614–626. [PubMed: 26551758]
24. Van Rooijen N. The liposome-mediated macrophage 'suicide' technique. J Immunol Methods. 1989; 124:1–6. [PubMed: 2530286]
25. Van Rooijen N, Sanders A. Liposome mediated depletion of macrophages: Mechanism of action, preparation of liposomes and applications. J Immunol Methods. 1994; 174:83–93. [PubMed: 8083541]
26. Bharat A, Chiu S, Zheng Z, Sun H, Yeldandi A, DeCamp MM, Perlman H, Budinger GR, Mohanakumar T. Lung-restricted antibodies mediate primary graft dysfunction and prevent allotolerance after murine lung transplantation. Am J Respir Cell Mol Biol. 2016; 55:532–541. [PubMed: 27144500]
27. Okazaki M, Krupnick AS, Kornfeld CG, Lai JM, Ritter JH, Richardson SB, Huang HJ, Das NA, Patterson GA, Gelman AE, Kreisel D. A mouse model of orthotopic vascularized aerated lung transplantation. Am J Transplant. 2007; 7:1672–1679. [PubMed: 17511692]
28. Krupnick AS, Lin X, Li W, Higashikubo R, Zinselmeyer BH, Hartzler H, Toth K, Ritter JH, Berezin MY, Wang ST, Miller MJ, Gelman AE, Kreisel D. Central memory CD8+ T lymphocytes mediate lung allograft acceptance. J Clin Invest. 2014; 124:1130–1143. [PubMed: 24569377]
29. Kreisel D, Sugimoto S, Tietjens J, Zhu J, Yamamoto S, Krupnick AS, Carmody RJ, Gelman AE. Bcl3 prevents acute inflammatory lung injury in mice by restraining emergency granulopoiesis. J Clin Invest. 2011; 121:265–276. [PubMed: 21157041]
30. Kreisel D, Sugimoto S, Zhu J, Nava R, Li W, Okazaki M, Yamamoto S, Ibrahim M, Huang HJ, Toth KA, Ritter JH, Krupnick AS, Miller MJ, Gelman AE. Emergency granulopoiesis promotes neutrophil-dendritic cell encounters that prevent mouse lung allograft acceptance. Blood. 2011; 118:6172–6182. [PubMed: 21972291]
31. Fong AM, Robinson LA, Steeber DA, Tedder TF, Yoshie O, Imai T, Patel DD. Fractalkine and CX_3CR1 mediate a novel mechanism of leukocyte capture, firm adhesion, and activation under physiologic flow. J Exp Med. 1998; 188:1413–1419. [PubMed: 9782118]
32. Hanna RN, Carlin LM, Hubbeling HG, Nackiewicz D, Green AM, Punt JA, Geissmann F, Hedrick CC. The transcription factor NR4A1 (Nur77) controls bone marrow differentiation and the survival of $Ly6C^-$ monocytes. Nat Immunol. 2011; 12:778–785. [PubMed: 21725321]
33. Anderson KG, Mayer-Barber K, Sung H, Beura L, James BR, Taylor JJ, Qunaj L, Griffith TS, Vezys V, Barber DL, Masopust D. Intravascular staining for discrimination of vascular and tissue leukocytes. Nat Protoc. 2014; 9:209–222. [PubMed: 24385150]
34. Patel BV, Tatham KC, Wilson MR, O'Dea KP, Takata M. In vivo compartmental analysis of leukocytes in mouse lungs. Am J Physiol Lung Cell Mol Physiol. 2015; 309:L639–L652. [PubMed: 26254421]
35. Feng L, Xia Y, Yoshimura T, Wilson CB. Modulation of neutrophil influx in glomerulonephritis in the rat with anti-macrophage inflammatory protein-2 (MIP-2) antibody. J Clin Invest. 1995; 95:1009–1017. [PubMed: 7883948]
36. Reutershan J, Morris MA, Burcin TL, Smith DF, Chang D, Saprito MS, Ley K. Critical role of endothelial CXCR2 in LPS-induced neutrophil migration into the lung. J Clin Invest. 2006; 116:695–702. [PubMed: 16485040]
37. Spahn JH, Li W, Bribriesco AC, Liu J, Shen H, Ibricevic A, Pan J-H, Zinselmeyer BH, Brody SL, Goldstein DR, Krupnick AS, Gelman AE, Miller MJ, Kreisel D. DAP12 expression in lung

macrophages mediates ischemia/reperfusion injury by promoting neutrophil extravasation. J Immunol. 2015; 194:4039–4048. [PubMed: 25762783]

38. McKenzie CG, Kim M, Singh TK, Milev Y, Freedman J, Semple JW. Peripheral blood monocyte-derived chemokine blockade prevents murine transfusion-related acute lung injury (TRALI). Blood. 2014; 123:3496–3503. [PubMed: 24637362]
39. Jones SA, Dewald B, Clark-Lewis I, Baggiolini M. Chemokine antagonists that discriminate between interleukin-8 receptors. Selective blockers of CXCR2. J Biol Chem. 1997; 272:16166–16169. [PubMed: 9195914]
40. Casilli F, Bianchini A, Gloaguen I, Biordi L, Alesse E, Festuccia C, Cavalieri B, Strippoli R, Cervellera MN, Di Bitondo R, Ferretti E, Mainiero F, Bizzarri C, Colotta F, Bertini R. Inhibition of interleukin-8 (CXCL8/IL-8) responses by repertaxin, a new inhibitor of the chemokine receptors CXCR1 and CXCR2. Biochem Pharmacol. 2005; 69:385–394. [PubMed: 15652230]
41. Thomas G, Tacke R, Hedrick CC, Hanna RN. Nonclassical patrolling monocyte function in the vasculature. Arterioscler Thromb Vasc Biol. 2015; 35:1306–1316. [PubMed: 25838429]
42. Ginhoux F, Jung S. Monocytes and macrophages: Developmental pathways and tissue homeostasis. Nat Rev Immunol. 2014; 14:392–404. [PubMed: 24854589]
43. Sunderkotter C, Nikolic T, Dillon MJ, Van Rooijen N, Stehling M, Drevets DA, Leenen PJM. Subpopulations of mouse blood monocytes differ in maturation stage and inflammatory response. J Immunol. 2004; 172:4410–4417. [PubMed: 15034056]
44. Jung S, Aliberti J, Graemmel P, Sunshine MJ, Kreutzberg GW, Sher A, Littman DR. Analysis of fractalkine receptor CX_3CR1 function by targeted deletion and green fluorescent protein reporter gene insertion. Mol Cell Biol. 2000; 20:4106–4114. [PubMed: 10805752]
45. Yona S, Kim K-W, Wolf Y, Mildner A, Varol D, Breker M, Strauss-Ayali D, Viukov S, Guilliams M, Misharin A, Hume DA, Perlman H, Malissen B, Zelzer E, Jung S. Fate mapping reveals origins and dynamics of monocytes and tissue macrophages under homeostasis. Immunity. 2013; 38:79–91. [PubMed: 23273845]
46. Bazan JF, Bacon KB, Hardiman G, Wang W, Soo K, Rossi D, Greaves DR, Zlotnik A, Schall TJ. A new class of membrane-bound chemokine with a CX_3C motif. Nature. 1997; 385:640–644. [PubMed: 9024663]
47. Oh D-J, Dursun B, He Z, Lu L, Hoke TS, Ljubanovic D, Faubel S, Edelstein CL. Fractalkine receptor (CX_3CR1) inhibition is protective against ischemic acute renal failure in mice. Am J Physiol Renal Physiol. 2008; 294:F264–F271. [PubMed: 18003857]
48. Dhaliwal K, Scholefield E, Ferenbach D, Gibbons M, Duffin R, Dorward DA, Morris AC, Humphries D, MacKinnon A, Wilkinson TS, Wallace WAH, van Rooijen N, Mack M, Rossi AG, Davidson DJ, Hirani N, Hughes J, Haslett C, Simpson AJ. Monocytes control second-phase neutrophil emigration in established lipopolysaccharide-induced murine lung injury. Am J Respir Crit Care Med. 2012; 186:514–524. [PubMed: 22822022]
49. Carlin LM, Auffray C, Geissmann F. Measuring intravascular migration of mouse $Ly6C^{low}$ monocytes in vivo using intravital microscopy. Curr Protoc Immunol. 2013; 14:11–16.
50. Leifer CA, Medvedev AE. Molecular mechanisms of regulation of Toll-like receptor signaling. J Leukoc Biol. 2016; 100:927–941. [PubMed: 27343013]
51. Rodan GA, Fleisch HA. Bisphosphonates: Mechanisms of action. J Clin Invest. 1996; 97:2692–2696. [PubMed: 8675678]
52. Orens JB, Boehler A, de Perrot M, Estenne M, Glanville AR, Keshavjee S, Kotloff R, Morton J, Studer SM, Van Raemdonck D, Waddel T, Snell; GI. Pulmonary Council, International Society for Heart and Lung Transplantation, A review of lung transplant donor acceptability criteria. J Heart Lung Transpl. 2003; 22:1183–1200.
53. Pasque MK. Standardizing thoracic organ procurement for transplantation. J Thorac Cardiovasc Surg. 2010; 139:13–17. [PubMed: 20106357]
54. Nayak DK, Zhou F, Xu M, Huang J, Tsuji M, Hachem R, Mohanakumar T. Long-term persistence of donor alveolar macrophages in human lung transplant recipients that influences donor-specific immune responses. Am J Transplant. 2016; 16:2300–2311. [PubMed: 27062199]

55. Zheng Z, Wang J, Huang X, Jiang K, Nie J, Qiao X, Li J. Improvements of the surgical technique on the established mouse model of orthotopic single lung transplantation. PLOS ONE. 2013; 8:e81000. [PubMed: 24278363]

56. Misharin AV, Morales-Nebreda L, Mutlu GM, Budinger GR, Perlman H. Flow cytometric analysis of macrophages and dendritic cell subsets in the mouse lung. Am J Respir Cell Mol Biol. 2013; 49:503–510. [PubMed: 23672262]

57. Eden E, Navon R, Steinfeld I, Lipson D, Yakhini Z. *GOrilla*: A tool for discovery and visualization of enriched GO terms in ranked gene lists. BMC Bioinf. 2009; 10:48.

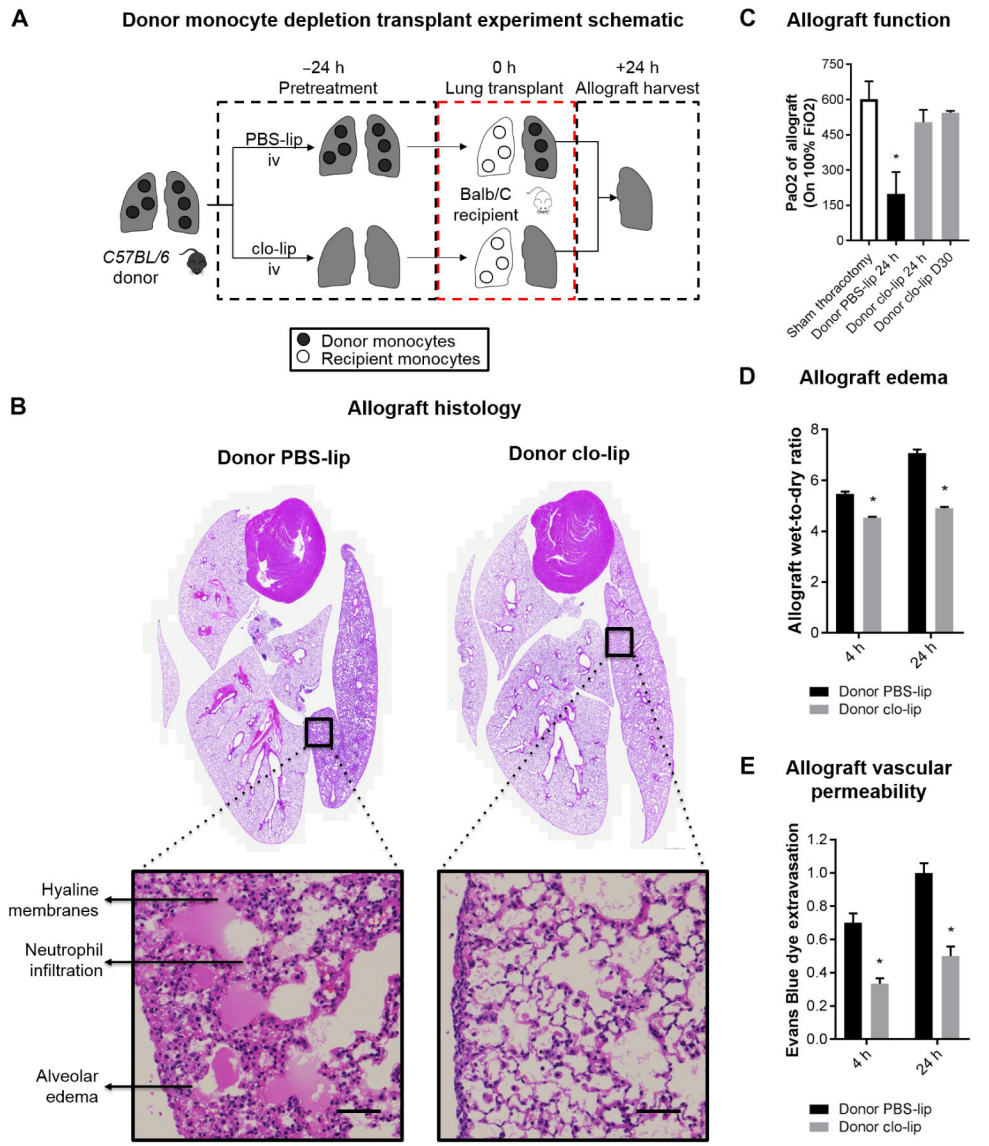

Fig. 1. Donor intravenous clo-lip treatment ameliorates PGD after transplantation

(**A**) Experimental design. (**B**) Allograft histology. Representative histology of the heart-lung blocks of control PBS-lip and intravenous (iv) clo-lip–treated donors at 24 hours after reperfusion. Hematoxylin and eosin staining. Inset scale bars, 50 μm. (**C**) Allograft function measured by PaO_2 on 100% FiO_2 as a marker of lung injury at 24 hours after transplant. *P = 0.01, n = 3 to 6 per group. (**D**) Allograft edema measured by wet-to-dry ratio of allograft at 4 and 24 hours after reperfusion. *P < 0.001, n = 5 per group. (**E**) Allograft vascular permeability measured by Evans blue dye extravasation leak test of allograft at 4 and 24 hours after reperfusion. *P < 0.01, n = 5 per group. Unpaired Student's t test was used to compare means.

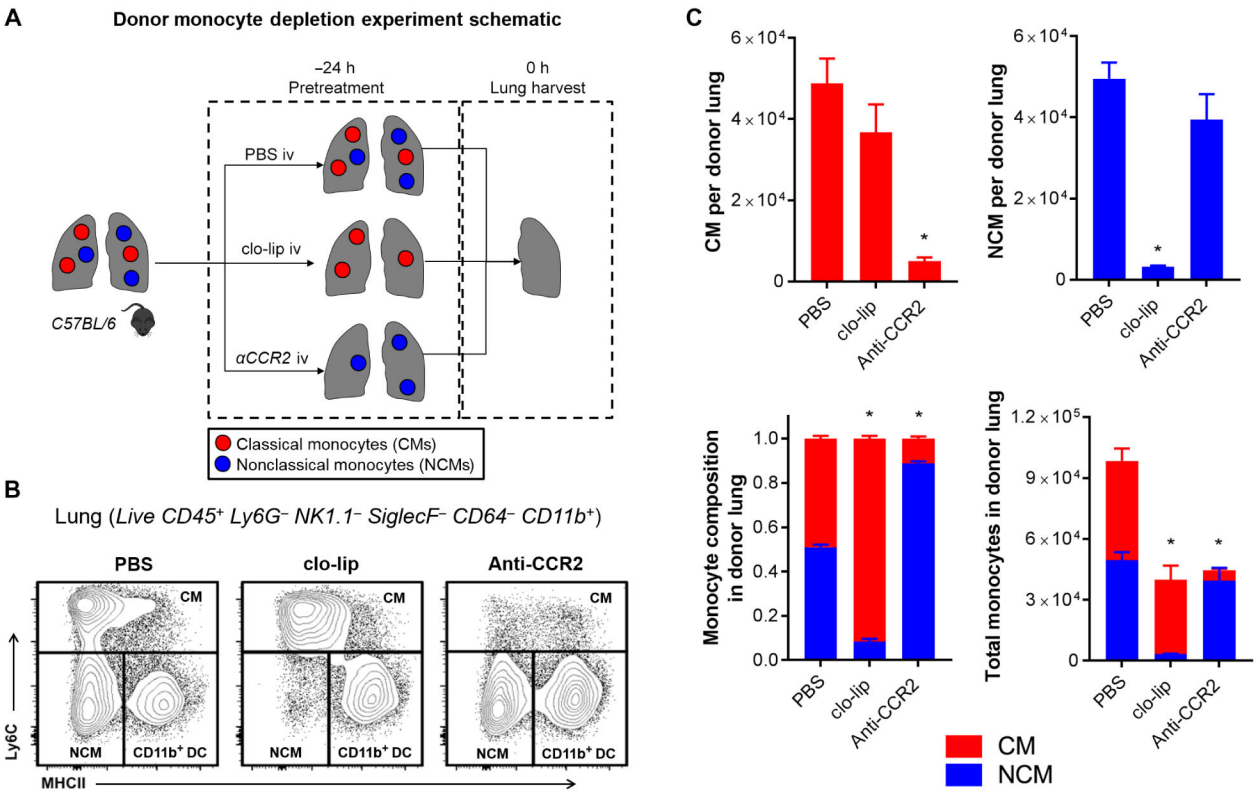

Fig. 2. Intravenous clo-lip selectively depletes NCMs in donor lungs

(**A**) Experimental design. (**B**) Flow cytometry plots showing effects of monocyte depletion strategies on CMs, NCMs, and CD11b$^+$ dendritic cells (DCs) in wild-type (WT) mice (full gating strategy is shown in fig. S2). (**C**) Effects of clo-lip and anti-CCR2 on the number of monocytes and relative composition of lung monocytes at 24 hours after treatment. *$P <$ 0.01, $n = 5$ per group. (C) Data are representative of five experiments. Unpaired Student's t test with Holm-Šidák correction for multiple comparisons was used to compare means.

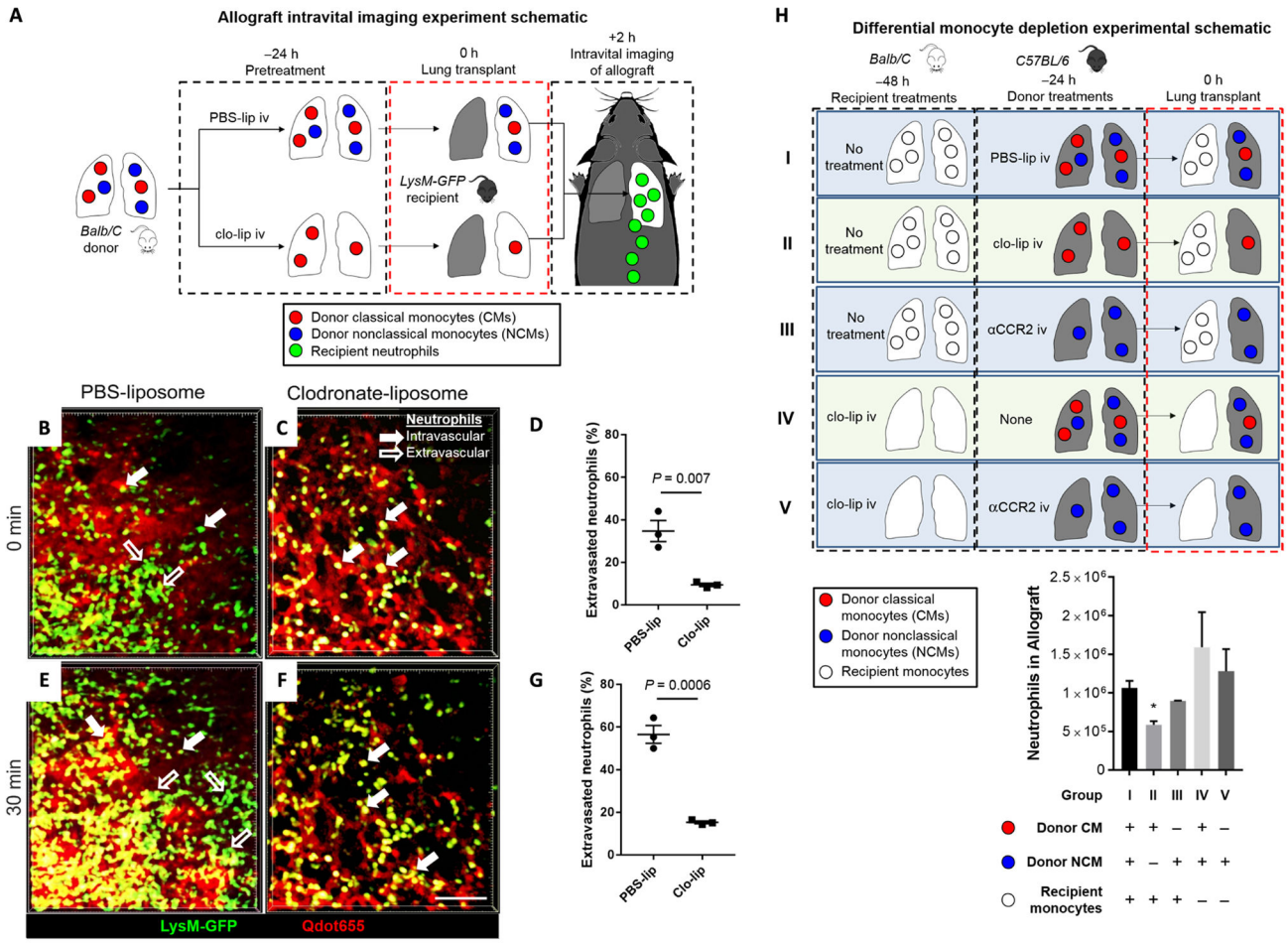

Fig. 3. Influx of recipient neutrophils into the allograft is abrogated by depletion of donor NCMs

(**A**) Experimental design. (**B** to **G**) Intravital two-photon imaging at 2 hours, starting at $t = 0$ min through $t = 30$ min after reperfusion. Representative still images of control PBS-lip–treated donor allograft immediately after reperfusion (also refer to movies S1 and S2). Green, LysM$^+$; red, Qdot655 blood vessels. Unpaired Student's t test was used to compare means. Scale bar, 50 μm. (**H**) Experimental design and result of differential monocyte depletion strategies in donors and recipients. Combinations of donor and recipient treatments were used to selectively deplete the different monocyte populations. The allograft was harvested at 24 hours after transplantation, and neutrophil influx was determined using flow cytometry. *$P = 0.001$ compared to group I (all other comparisons to group I are not significant), $n = 6$ per group. Unpaired Student's t test with Holm-Šidák correction for multiple comparisons was used to compare means.

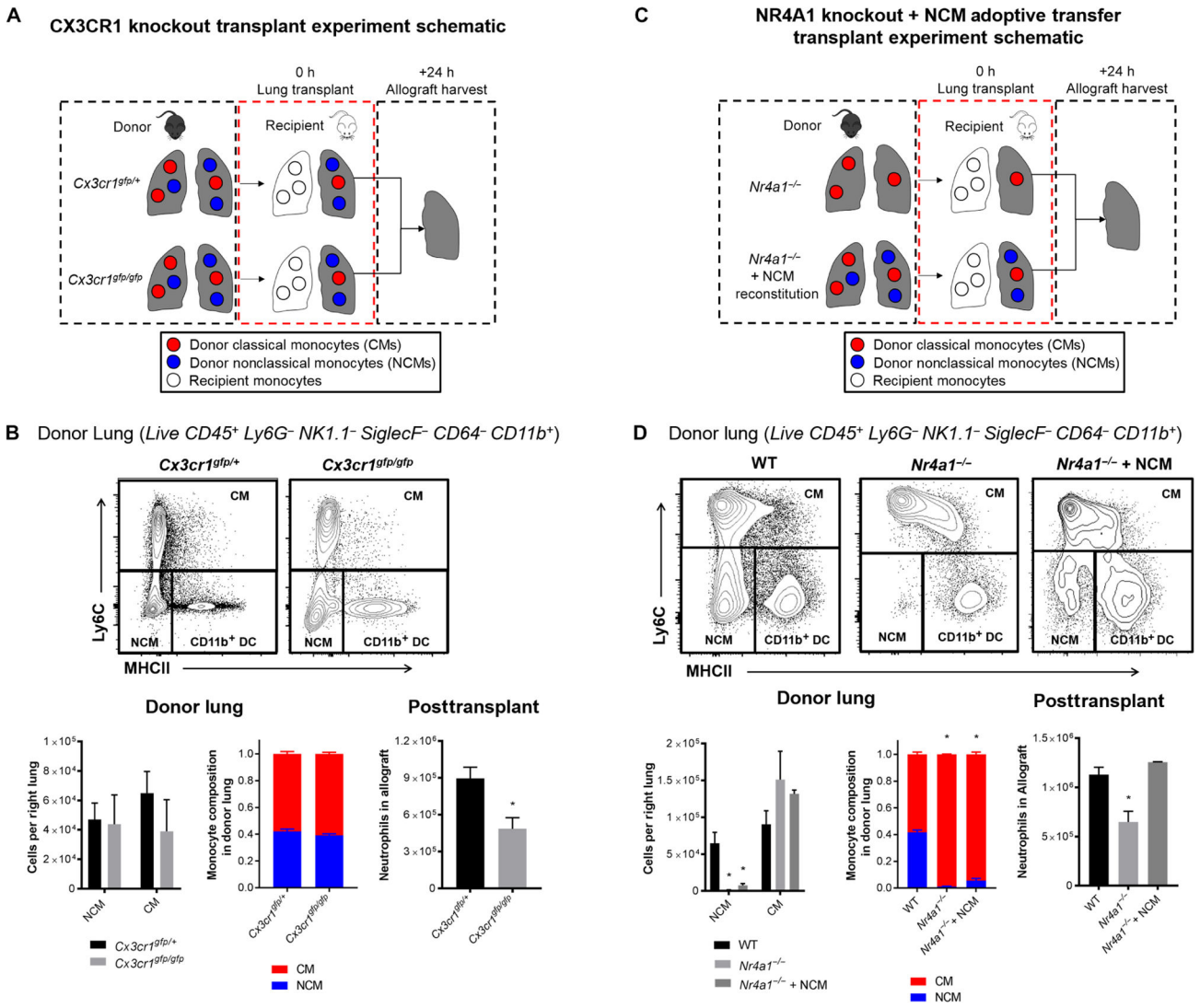

Fig. 4. Pulmonary intravascular NCMs are dependent on CX3CR1 to recruit neutrophils, and reconstitution of depleted NCMs restores neutrophil influx in NR4A1-deficient mice

(**A**) Experimental design for CX3CR1 knockout transplants. (**B**) Representative flow plots and effects of CX3CR1 deletion on monocyte populations in donor lungs and posttransplant neutrophil infiltration of the allograft. **P* = 0.01, *n* = 6 per group. Unpaired Student's *t* test was used to compare means. (**C**) Experimental design for NR4A1 knockout transplants. (**D**) Representative flow plots and effects of NR4A1 deletion NCM reconstitution on monocyte populations in donor lungs and posttransplant neutrophil infiltration. **P* = 0.01, *n* = 5 per group. Unpaired Student's *t* test with Holm-Šidák correction for multiple comparisons was used to compare means.

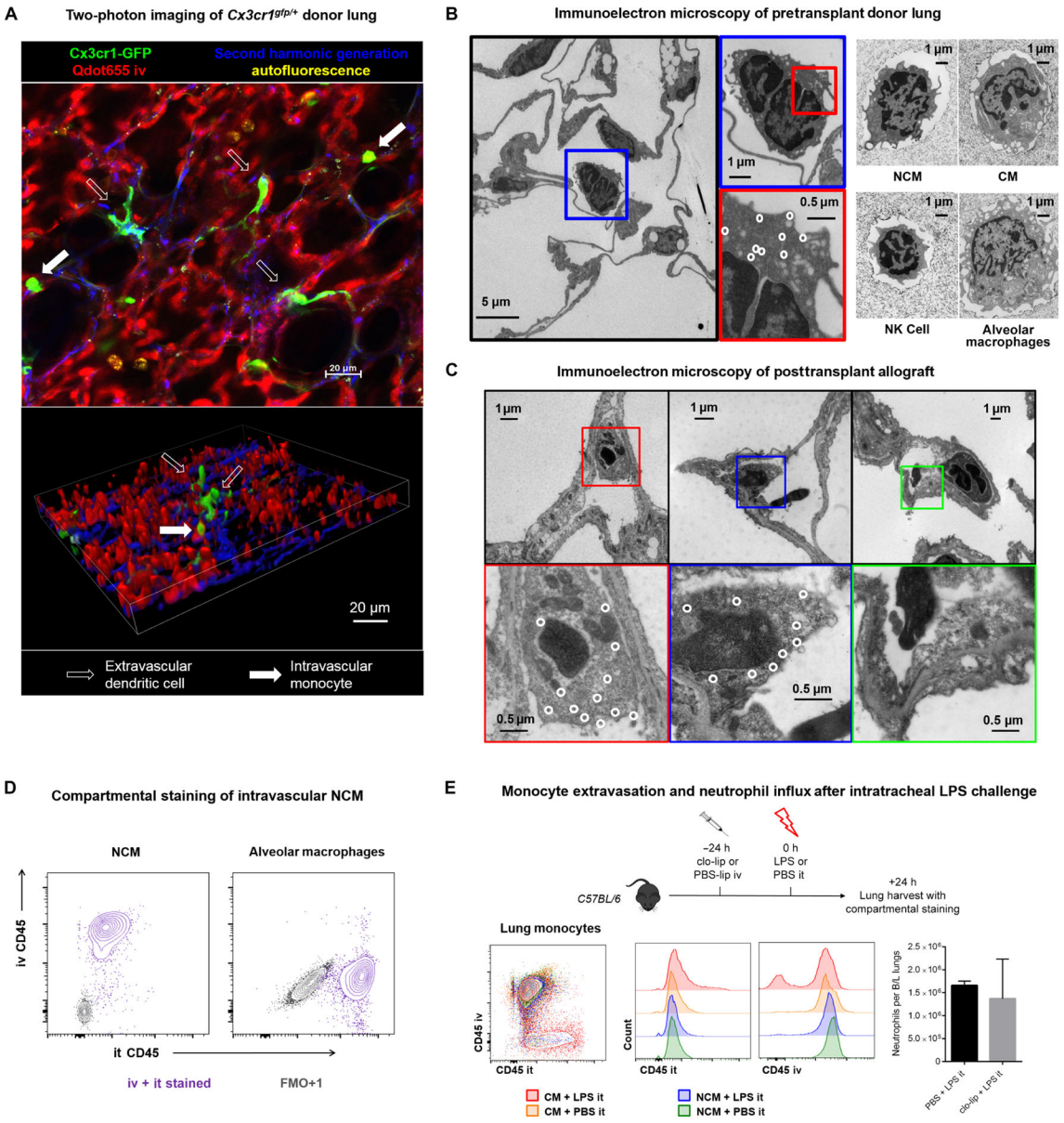

Fig. 5. Compartmentalization of pulmonary NCMs and CMs and their response to intratracheal lipopolysaccharide

(**A**) Two-photon imaging of Cx3cr1$^{gfp/+}$ lungs. Green, Cx3cr1^{+}; red, Qdot655 blood vessels; blue, second harmonic generation collagen; yellow, autofluorescent alveolar macrophages. Filled arrow, intravascular cell; open arrow, extravascular cell. (**B**) Morphology of the lung myeloid cell populations in the donor lung using immunogold electron microscopy in the Cx3cr1$^{gfp/+}$ reporter mouse. Left: Immunoelectron microscopy of fixed Cx3cr1$^{gfp/+}$ lung, with white circles highlighting gold nanoparticles staining for GFP. Right: Electron microscopy micrographs of postsort cells from WT B6 mouse lung. (**C**) Immunoelectron microscopy of Cx3cr1$^{gfp/+}$ donor lungs at 4 hours after reperfusion, with white circles highlighting gold nanoparticles staining for GFP. Left and middle: NCMs bound to the endothelium with areas of exposed, thickened basement membrane and endothelial cell

blebbing. Right: Neutrophil bound to the endothelium in the vicinity of a blebbing endothelial cell. (**D**) Representative compartmental staining of NCMs and alveolar macrophages. As negative control, FMO+1 (fluorescence minus one control + 1) staining is shown. it, intratracheal. (**E**) Experimental design and representative flow diagrams of intravenous and intratracheal anti-CD45 staining in LPS-treated and control mice along with neutrophil infiltration into the lungs with and without intravenous clo-lip pretreatment. Unpaired Student's *t* test, not significant. $n = 5$ per group. LPS, lipopolysaccharide.

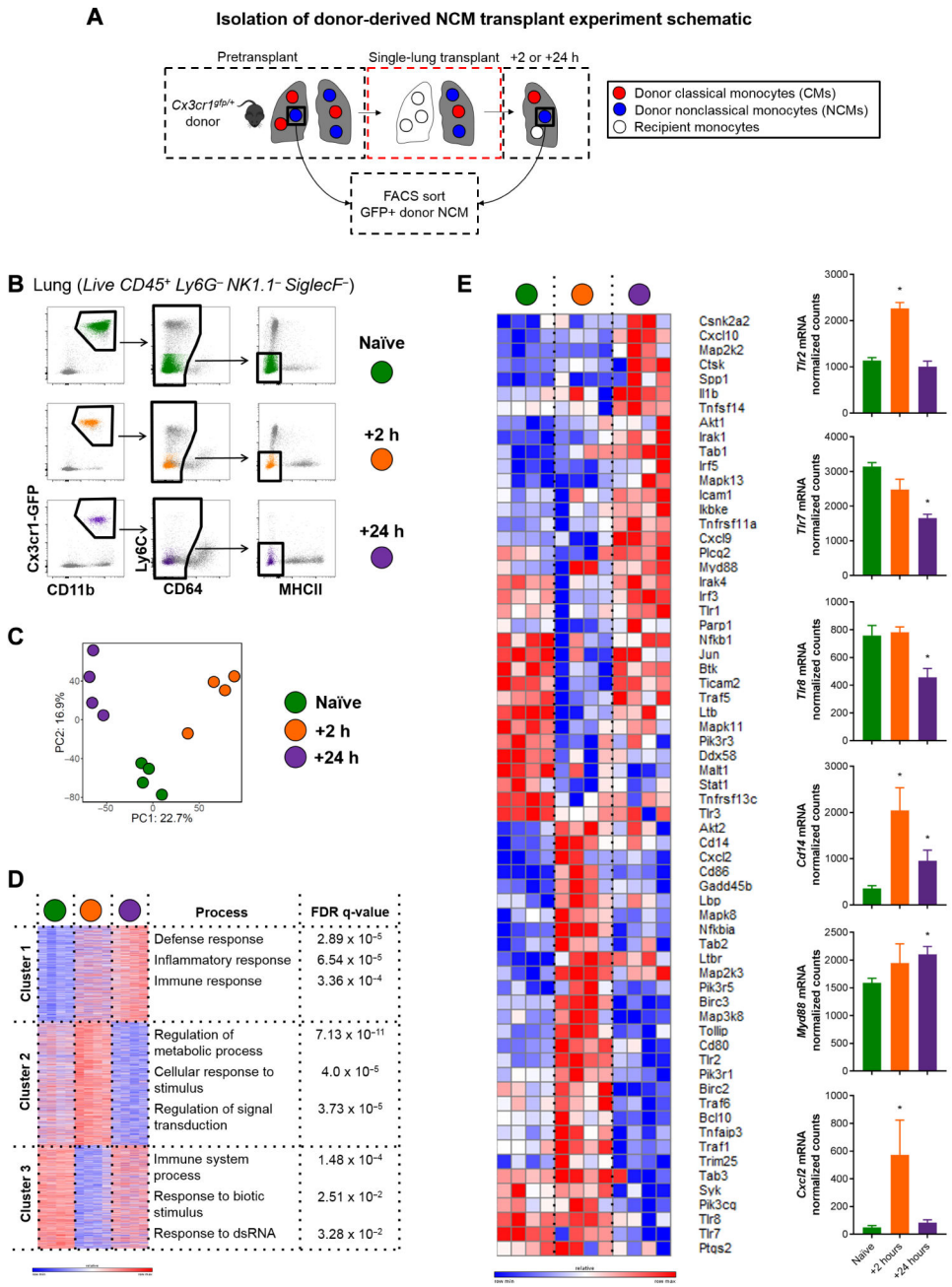

Fig. 6. Transcriptional profiling of murine posttransplant donor-derived NCMs

(**A**) Experimental plan to isolate and sort NCMs from donor-naïve, +2-hour, and +24-hour posttransplant lung. (**B**) Sorting strategy with representative flow plots from each time point. (**C**) Principle components (PC) analysis of samples. (**D**) Gene ontology process enrichment analysis using K-means clustering. (**E**) TLR and nuclear factor κB signaling pathway genes, which were differentially expressed by cutoff of adjusted *P* value of <0.05 by pairwise comparison between time points, with the normalized counts of genes of interest depicted. **P* < 0.04 by one-way analysis of variance (ANOVA), *n* = 4 per group. Heat map scale bars represent $\log_2$ scale.

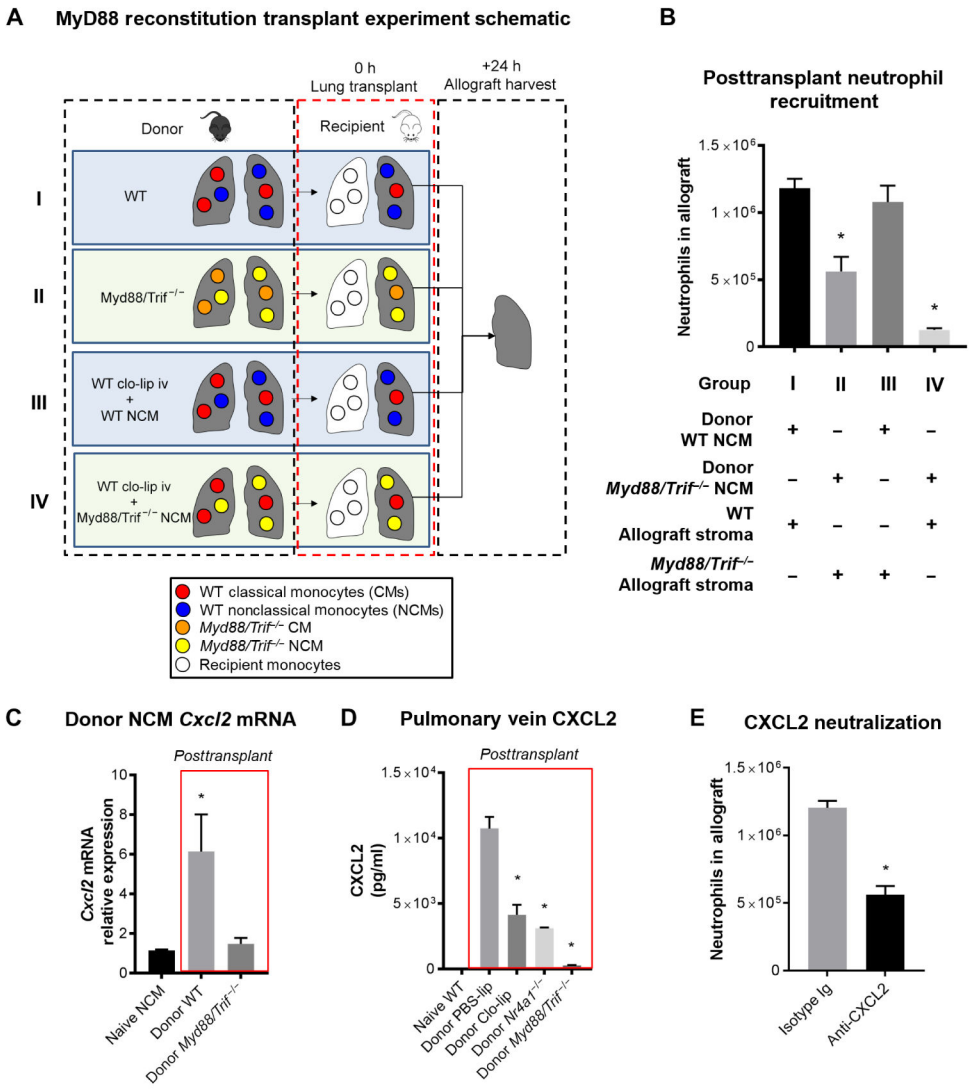

Fig. 7. NCMs are dependent on MyD88/TRIF signaling to produce CXCL2

(**A**) Experimental design. (**B**) Effects of reconstitution of NCM-depleted donor lungs with either WT or *Myd88/Trif*$^{-/-}$ NCMs. *$P < 0.01$, $n = 5$ per group. (**C**) *Cxcl2* transcript expression level in donor-derived NCMs measured by quantitative polymerase chain reaction at 2 hours after transplant. As control, the baseline expression of *Cxcl2* in WT pulmonary NCMs is shown. *$P = 0.01$. (**D**) Effect of NCM depletion on CXCL2 cytokine levels in allograft circulation when NCMs are depleted. As control, the CXCL2 levels in left pulmonary vein blood of WT mice are shown. *$P < 0.01$, $n = 5$ per group. Unpaired Student's *t* test with Holm-Šidák correction for multiple comparisons was used to compare means. (**E**) Effect of CXCL2 blockade on neutrophil recruitment in the recipient at 24 hours after transplant. *$P = 0.001$, $n = 5$ per group. Unpaired Student's *t* test was used to compare means.

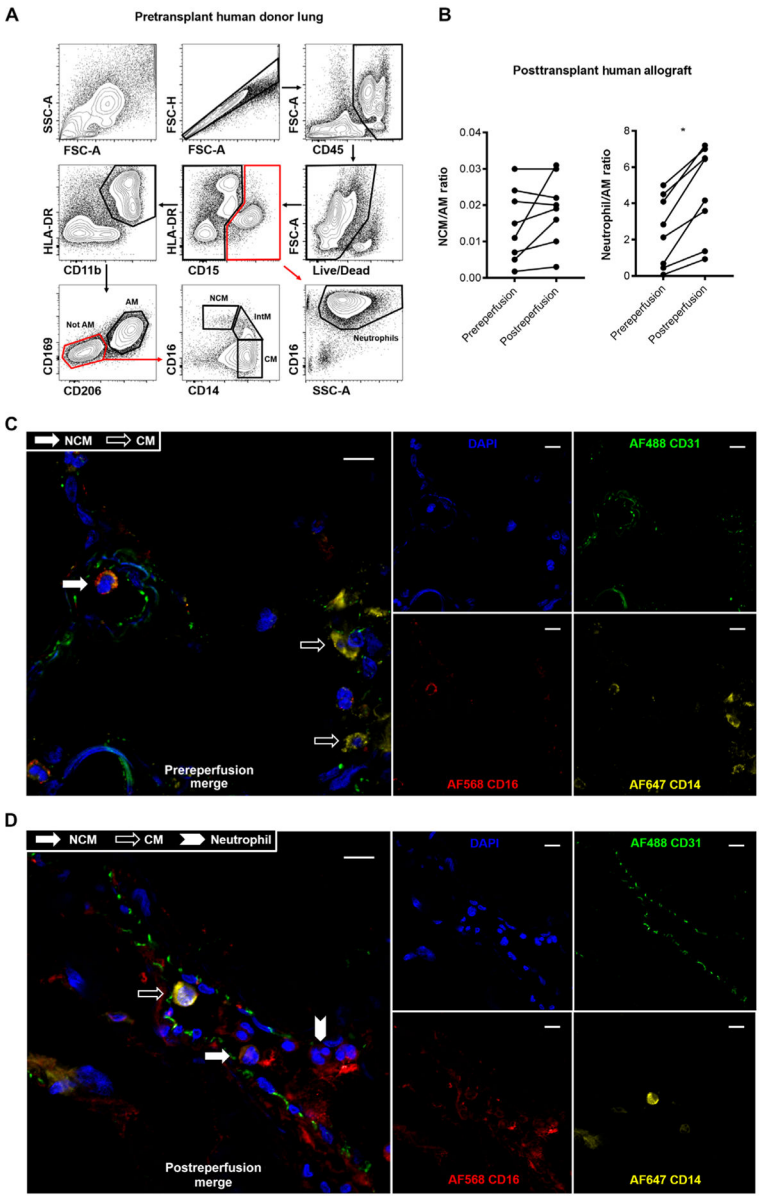

Fig. 8. Myeloid cell populations in human donor lungs and immediate postreperfusion changes

(**A**) Representative gating strategy of human lungs flushed and used in clinical transplantation. After excluding doublets and dead cells, and including only $CD45^+$ cells, neutrophils were identified as $CD15^+CD16^+SSC^{high}$. After gating out $CD15^+$ events, an $HLA\text{-}DR^+CD11b^+$ gate was used to identify monocytes and macrophages. Alveolar macrophages (AMs) were identified as $CD15^-HLA\text{-}DR^+CD11b^+CD169^+CD206^+$. After gating out AMs, NCMs were identified as $CD16^{++}CD14^{dim}$, intermediate monocytes (IntMs) as $CD16^+CD14^+$, and CMs as $CD14^+CD16^-$. (**B**) Changes in NCMs and neutrophils at 90 min after reperfusion. Data are expressed as cell count per AM to standardize across patients. Biopsies were taken serially from the same location in the lung. $*P = 0.02$ (by paired Student's t test), $n = 8$. Immunofluoresence microscopy of prereperfusion (**C**) and postreperfusion (**D**) human lung samples depicting endothelial-bound intravascular

$CD16^{+}CD14^{dim}$ NCMs (filled white arrow) in contrast with $CD16^{-}$ $CD14^{high}$ CMs (open arrow) and $CD16^{+}CD14^{+}$ neutrophils (filled white chevron). Green, CD31; blue, DAPI (4′, 6-diamidino-2-phenylindole); red, CD16; yellow, CD14. Scale bars, 10 μm.